

# Advancing offshore solar energy generation: The HelioSea concept

Mario López<sup>a,\*</sup>, Rubén Claus<sup>a</sup>, Fernando Soto<sup>a</sup>, Zenaida A. Hernández-Garrastacho<sup>a</sup>, Alejandro Cebada-Relea<sup>a</sup>, Orlando Simancas<sup>b</sup>

<sup>a</sup> DyMAST Research Group and CUIDA Research Centre, Polytechnic School of Mieres - University of Oviedo, 33600 Mieres, Asturias, Spain

<sup>b</sup> Asturmadi Reneergy SL, Travesía de la Industria, 51, 33401 Avilés, Asturias, Spain

## HIGHLIGHTS

- HelioSea is a floating PV system specially designed for offshore conditions.
- HelioSea innovatively merges tension leg platform with dual-axis tracker.
- HelioSea reduces pitch motions, ensuring PV module alignment.
- HelioSea withstands 5 m waves and 30 m/s winds.
- HelioSea's LCOE ranges from 160 to 270 €/MWh.

## ARTICLE INFO

### Keywords:

Floating photovoltaic system  
FPV  
Offshore  
Marine renewable energy  
Ocean energy  
Tension leg platform

## ABSTRACT

HelioSea is an innovative offshore solar energy concept that combines a dual-axis tracking system and a tension leg platform (TLP) to maximize electricity generation and ensure structural reliability in challenging marine environments. The tracker enhances energy generation by optimizing solar irradiance throughout the year, while also raising solar modules above the water surface to avoid wave impact and enhance cooling efficiency. The TLP provides stability and minimizes wave loading on the structure, ensuring that the photovoltaic panels maintain their optimal orientations, even under severe conditions. Numerical simulation reveals that relative pitch amplitudes are almost insignificant, with values of 0.6 deg. for waves with a height of 5 m and winds of 30 m/s. Structural assessment shows robust safety factors, with potential for optimization in certain components. The levelized cost of energy (LCOE) of HelioSea would range between 160 and 270 €/MWh. Bearing in mind the incipient stage of development of this technology and the cost of other offshore energy systems, the proposed concept can be considered a promising solution for offshore solar energy. To further enhance this conceptual design, future stages should include experimental proof-of-concept to refine geometry, materials, and ultimately, the cost of energy.

## 1. Introduction

Solar energy stands as one of the most promising technologies to replace all the conventional energy sources, owing to its abundance, cleanliness, cost-effectiveness, and inexhaustive nature [1]. Particularly, solar photovoltaic (PV) energy is forecasted to be the leading renewable due to its potential to fulfil the global energy demand and the recent decline in the associated technology costs [2]. Nevertheless, large-scale and ground-mounted PV (GPV) generation demands large amounts of land that could otherwise benefit from other uses [3].

To address the increasing demand for land of solar energy, floating

PV (FPV) technology has experienced a significant growth over the past decade [4]. Commercial FPV technologies have been effectively deployed worldwide, predominantly in onshore freshwater bodies, where the wave exposure is minimal. The key components of any FPV system consist of: PV modules to harvest the solar energy, a floating system to provide buoyancy, a mooring system that forestalls the free movement of the plant and electrical components utilized to transform and transport electricity.

FPV plants offer several advantages over their GPV counterparts:

\* Corresponding author.

E-mail address: [mario.lopez@uniovi.es](mailto:mario.lopez@uniovi.es) (M. López).

<https://doi.org/10.1016/j.apenergy.2024.122710>

Received 17 October 2023; Received in revised form 4 December 2023; Accepted 21 January 2024

Available online 4 February 2024

0306-2619/© 2024 The Authors. Published by Elsevier Ltd. This is an open access article under the CC BY-NC license (<http://creativecommons.org/licenses/by-nc/4.0/>).

- The efficiency of PV panels is enhanced due to a cooler environment [5].
- The presence of water facilitates regular cleaning, mitigating soiling losses [6].
- Shading losses are minimized due to the open nature of water surfaces [7].
- Freshwater deployments offer the benefits of minimizing evaporation losses [8] and prevention of excessive algae growth [9].

Despite these advantages of FPV, with a levelized cost of energy (LCOE) ranging from 50 to 96 €/MWh, it remains higher than that GPV, which typically range from 35 to 40 €/MWh [5]. On another note, the application of FPV in freshwater is constrained by the availability of water bodies and their seasonal water level variations [10]. Consequently, there is a growing interest in harnessing the solar energy resource on the vast and unoccupied surfaces of oceans [11] (Fig. 1).

In offshore environments, FPV systems show potential for contributing to the decarbonization of shipping and synergizing with other marine activities and renewable systems [12]. For instance, floating offshore wind energy represents a technology with an LCOE ranging from 95 to 160 €/MWh, currently standing as one of the most promising marine renewable energy technologies [13]. The combination of offshore wind and solar has proven beneficial for smoothing power output and increasing the specific yield and capacity factor [14]. Other marine renewables may also benefit from such synergies [15]. For example, wave and tidal energy present significant theoretical potentials; however, their LCOE estimates remain high, ranging between 225 and 1750 €/MWh and between 255 and 910 €/MWh, respectively [16].

In the transition of FPV to offshore, the primary challenge lies in developing cost-effective technologies capable of withstanding the harsh environmental conditions. While salt deposits on solar panels seem to be non-critical [17], the combined impact of extreme waves and wind conditions could significantly impact the survivability and operation of these structures. In light of this issue, a multitude of concepts have been proposed (Fig. 2), most of them presenting a flexible and/or modular design, similar to those effectively applied in freshwater environments [18]. While several rigid FPV systems are currently under development, the availability of information is limited, possibly due to industrial property issues (e.g., [19]).

In this scenario, a novel offshore FPV system has been proposed: HelioSea (Fig. 1). This innovative concept leverages the combination of two distinct elements: a dual-axis solar tracker, maximizing solar energy generation, and a tension-leg platform (TLP), ensuring structural survivability, offering a stable platform, and simplifying towing and installation. The device is currently in its early stages of development, corresponding a technology readiness level (TRL) of 2 to 3.

The aims of this article are threefold. First, the main features of this

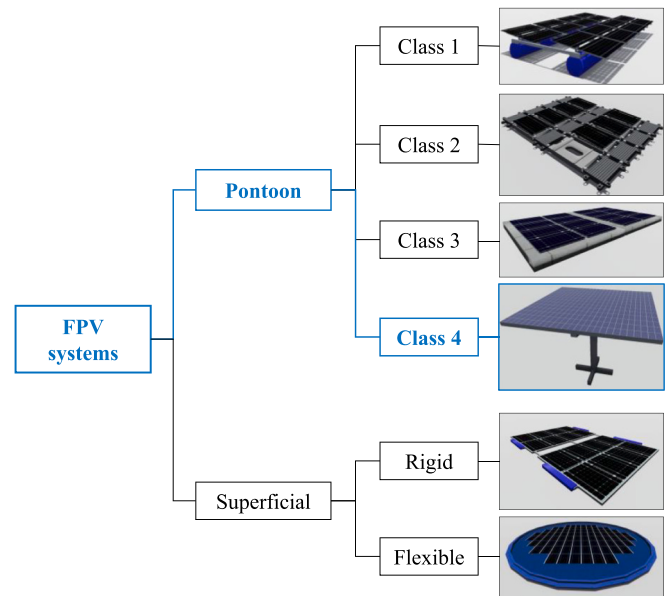


Fig. 2. Classification of FPV systems (adapted from [18]).

novel technology are presented for the first time through a comprehensive discussion of its advantages and limitations. Second, a proof-of-concept is carried out to assess the performance of the device in terms of structure and stability. To this purpose, a hydrodynamic numerical model is applied to simulate the performance of the device in operational and survival conditions. Third, a cost estimation is performed alongside a generation assessment to determine an approximated range of values for the LCOE. Based on these results, the article identifies the status of development and research needs for the technology.

The remainder of this paper is structured as follows. Section 2 provides a comprehensive description of the proposed offshore FPV system, highlighting its key features and components. In Section 3, the motion and structural analysis of the system are presented, preceded by an explanation of the testing and design conditions, along with the methods utilized in the analysis. An evaluation of the cost and energy production of the device for operating and survival conditions is presented in Section 4. Finally, Section 5 draws the main conclusions of the article and outlines future research directions.

## 2. Conceptual design and fundamentals

The HelioSea FPV system is divided into two well-differentiated parts or subsystems:

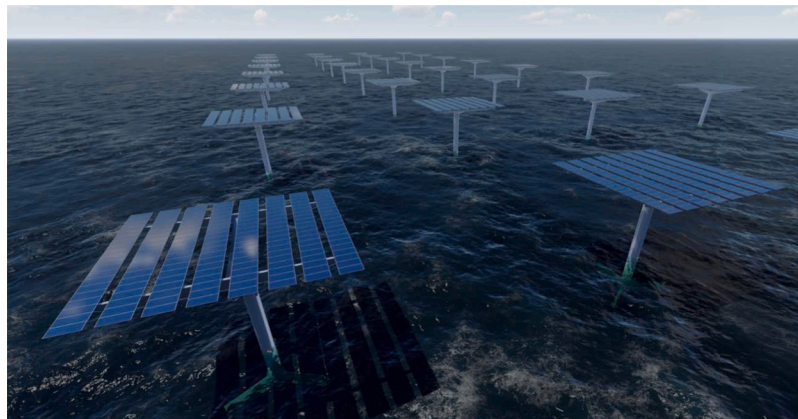
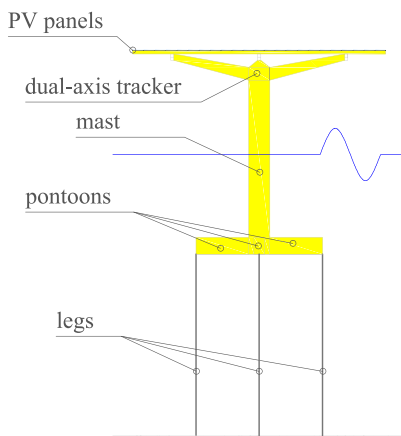


Fig. 1. Proposed offshore FPV system: main components (left panel) and a representation of an offshore solar farm (right panel).

- a substructure consisting of a mini tension leg platform (mini-TLP), and
- a superstructure that mounts a dual-axis solar tracker.

Both are presented hereinafter along with a discussion on the advantages they pose in terms of electricity generation potential and surviving the extreme environmental actions the ocean environment entails.

### 2.1. Substructure

The design of the substructure is based on the TLP, a type of technology that was developed for the extraction of oil and gas in offshore deep waters and that, more recently, has been applied to offshore wind turbines [20]. A typical TLP comprises a deck structure and a buoyant hull that is commonly composed vertical cylindrical columns, submerged horizontal pontoons, and, in some instances, tubular member bracing (Fig. 3). The key aspect is that the net buoyancy force exceeds the weight of the structure. This excess buoyancy is balanced with taut tendons or tethers, that vertically moor the floating platform. As a result, the TLP is compliant in the horizontal plane (i.e., it partially allows surge, sway, and yaw motions), while it restrains the vertical motions (pitch, heave, and roll). This feature ensures that the platform remains virtually horizontal with limited surge and sway excursions (Fig. 4). The TLPs present a series of advantages when compared to other offshore platforms, namely [21]:

- Mobile and reusable.
- Minimal vertical motion.
- Low increase in cost with increase in water depth.
- Deepwater capability.
- Low maintenance cost.

Regarding their disadvantages, those more relevant are:

- High initial cost.
- High subsea cost.
- Fatigue of tension.
- Difficult maintenance of subsea systems.

The proposed TLP consist of a mast or pole and four pontoons connected to the sea bottom through the corresponding taut mooring lines (the “legs”). Although previous research on offshore wind technology

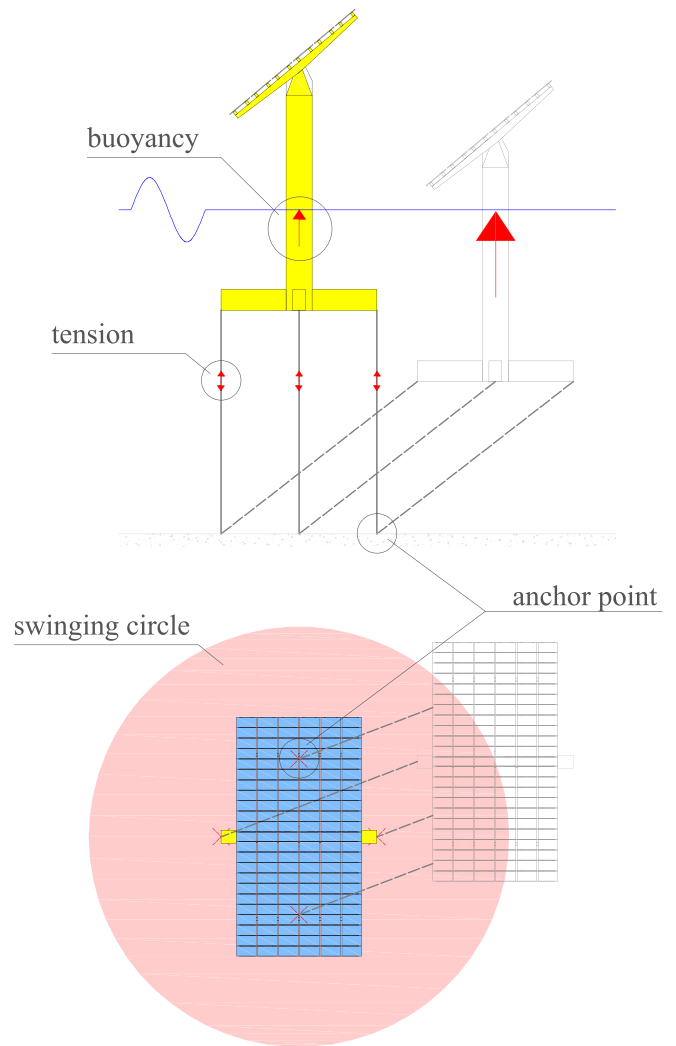


Fig. 4. Behaviour of the substructure – a tension leg platform (TLP). The movements of the platform are exaggerated for better interpretation.

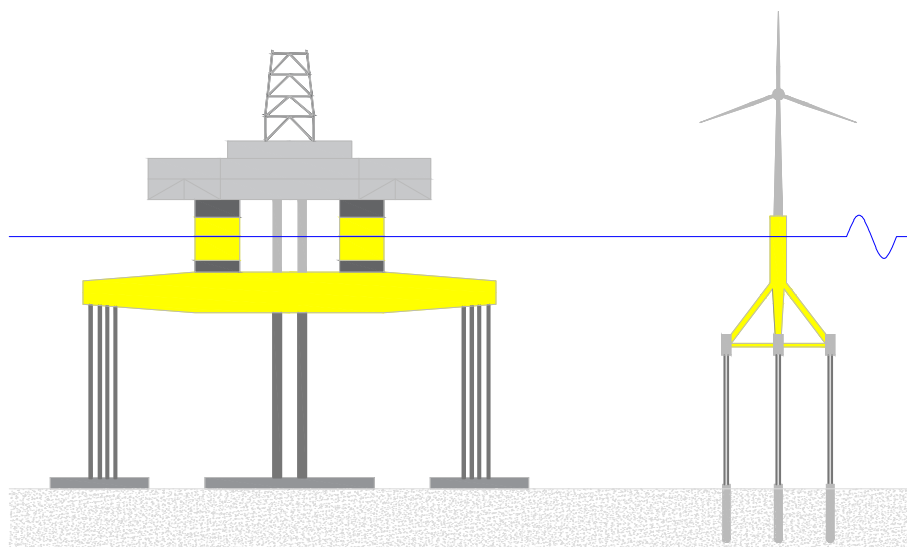


Fig. 3. Examples of tension leg platform (TLP) designs for oil and gas extraction (left) and for mounting an offshore wind turbine (right).

indicated that TLPs might entail a more complex installation process compared to alternative platforms such as semi-submersibles [22], there is an anticipated lower LCOE [23]. The advantages of integrating this substructure into a floating solar system are detailed and discussed below.

### 2.1.1. Structural performance

Offshore FPV applications should withstand much harsher environmental loads (due to tides, waves, and wind) than their counterparts in smaller freshwater bodies such as lakes and dam reservoirs. Therefore, the transition of solar energy generation to offshore requires the development of ad hoc floating structures. Several concepts have been proposed and are currently under development to achieve this objective, with two contrasting design strategies: flexible and rigid [18]. The former includes systems that rely on their compliance with waves, which results in lower internal stresses within the structure, while the latter strategy relies on the resistance of the structure to support the installation of PV panels [24]. The floating thin-film membrane proposed by Trapani et al. [25] is probably the most representative flexible design, while the SeaVolt concept is a good example of the rigid strategy [19]. Intermediate concepts include arrays of rigid floaters or pontoons with flexible connection systems, such as the soft-connected lattice-structure proposed by Jiang et al. [26] and the modular system developed by the company SolarDuck [27].

Flexible designs necessitate the use of thin-film technology, which is not yet cost-competitive with the low manufacturing costs of crystalline silicon technologies [28]. In the case of modular systems, prior experience has demonstrated that designing flexible connections remains a significant challenge that requires additional research and development efforts [29]. Until these challenges are addressed, floating structures without modular components and equipped with crystalline silicon solar cell panels may represent the most viable solution for the development of offshore FPV systems.

The proposed TLP substructure is independent and monolithic, thereby eliminating the requirement for mobile components and interconnections (apart from the mooring system). Although this feature offers structural advantages, it may also present a disadvantage in the design of offshore solar farms. To prevent collisions and allow maintenance, the standalone FPV units must be spaced at a specific horizontal distance (Fig. 1 and 4), which leads to a larger spatial footprint required for the same installed power – i.e., capacity density. However, considering the significantly higher specific yield of offshore solar energy (up to seven times greater than that of offshore wind according to reference [14]), it is unlikely that the potential impact of this concern will have a substantial effect on the feasibility of the concept.

### 2.1.2. Stability

The proposed substructure is intended to maximize the overall electricity generation by providing a stable platform to place the PV panels. Preventing rotational motions (pitch, roll and yaw) is crucial since the subsequent panel misalignments (tilt and azimuth) can substantially reduce the efficiency of PV modules [30]. A recent study focusing on the wave-induced motion of an FPV system revealed a decrease in sunlight exposure, particularly during pitch motions [31]. Another study, which focus on the use of decommissioned FPSOs as FPV plants, estimated great energy losses due to roll motions [32]. Some PV platforms were design so as to minimize the response to wave excitation and prevent panel misalignment [33]. The FPV response to waves is highly dependent on the design of the floating system itself. As previously mentioned, the TLP minimizes the wave-induced motions, and especially pitch.

## 2.2. Superstructure: Dual-axis solar tracker

The superstructure is based on the typical top-of-pole solar panel mount used in terrestrial solar energy projects. Its main function is

supporting the PV panels and accommodating the tracking systems as well as signal processing units, sensors, electromagnetic & mechanical motion control panels, and power supply systems, among other. The pole holds a base frame of beams with a second frame of beams mounted crossways. The PV panels are laid over the secondary beams.

While the concept is scalable, the proposed initial design mounts 138 bifacial PV panels with a rated power of  $P_{STC} = 545$  W (Table 1) in 6 rows of 23, which results in a 75-kW rated power unit. This selection was made as a compromise between structural integrity and total energy production. It is important to note that, based on previous experience with GPV systems, very large dual-axis solar trackers may face significant challenges with wind exposure.

The vertical and horizontal trackers automatically adjust two angles using servo motors throughout the day (Fig. 5):

- the solar panel's tilt angle, by rotating the base frame of beams from the horizontal plane ( $\alpha$ ), and
- the azimuth, or the direction the solar panels are facing, by rotating the superstructure with respect to the substructure ( $\beta$ ).

The HelioSea system maximizes the energy yield for a broad range of conditions and scenarios by combining tracking and bifacial panels. Future standardization and industrialization are expected to reduce the manufacturing costs of both technologies and, subsequently, the LCOE of HelioSea. The advantages of the proposed design and subsystems are discussed below.

### 2.2.1. Dual-axis tracker

Dual-axis trackers maximize the amount of direct normal irradiance (DNI) striking the front of PV arrays throughout the year. This results in an increased annual energy yield and a smoother power output throughout the day [34]. The simplest method for maximizing the insolation received by a PV panel is to mount it on a fixed frame that is tilted relative to the horizontal plane. Most FPV designs apply a fixed tilt angle equal to the local geographic latitude (also known as latitude tilt) and only a few systems include a tracking system (mostly single-axis vertical trackers, e.g., [35,36]). However, it is well known that tracking systems maximize the incident solar irradiance year-round. Considering previous studies on ground-mounted solar trackers, the energy return of single-axis and dual-axis trackers may reach 25% and 40%, respectively, when compared to the fixed PV systems [37]. Nonetheless, even though dual-axis solar tracking systems outperform their single-axis and fixed counterparts, they require a more intricate design with rotating components and control mechanisms. This entails a greater cost and maintenance requirements [38]. For this reason, different tracking strategies can minimize the LCOE depending on the latitude and environmental conditions of the installation site. In any case, dual-axis solar trackers are optimal in terms of maximizing the energy yield.

Another key difference from previous FPV concepts is that the top-of-the-pole configuration enables the PV panels to be installed at a sufficient height to protect them from extreme wave impacts, a major challenge for offshore applications (as discussed in Section 2.1.1). Although

**Table 1**  
Technical specifications of the reference PV module.

Parameter	Value	Units
$P_{STC}$	545	W
Efficiency	21.13	%
$\alpha_p$	-0.35	$^{\circ}\text{C}^{-1}$
Length	2.27	m
Width	1.13	m
Surface	1.95	$\text{m}^2$
Weight	28.9	kg
Material	P type monocrystalline	-
Manufacturer	Jinko Solar	-

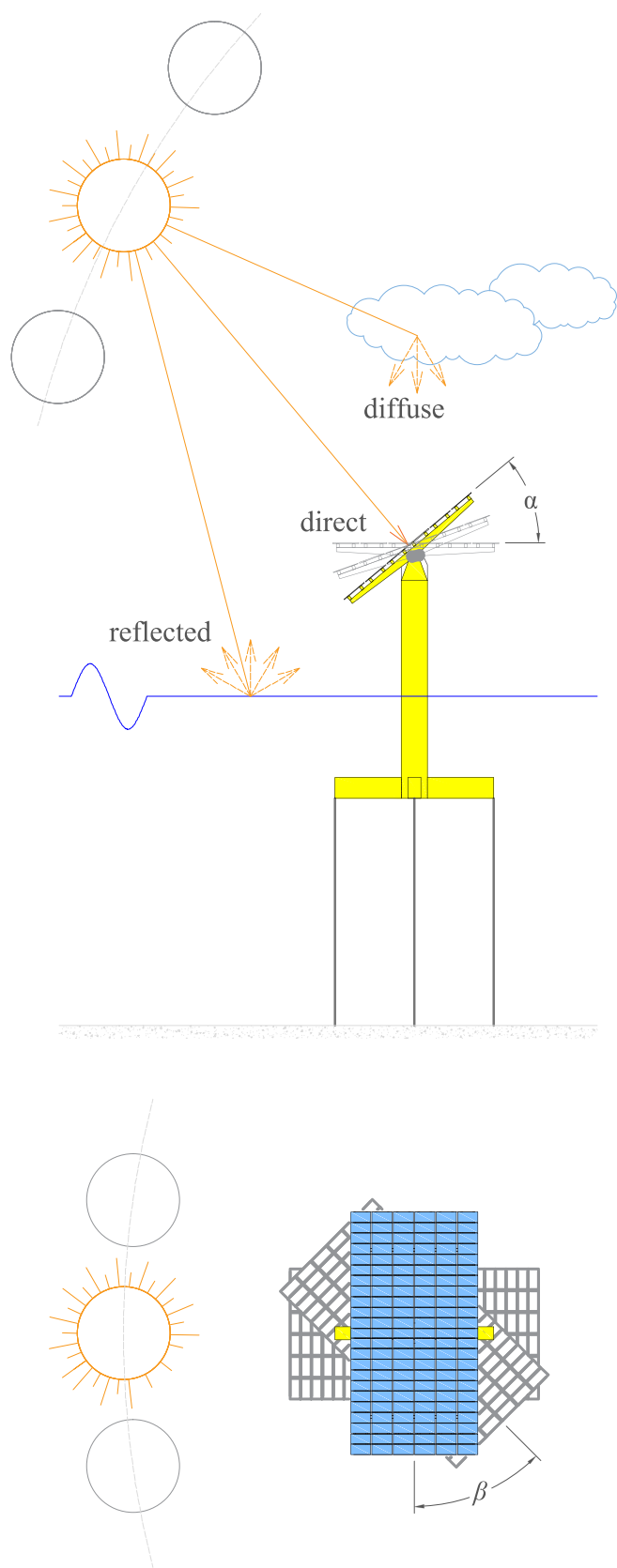


Fig. 5. Behaviour of the superstructure – a dual-axis solar tracker.

this feature may result in higher wind loads (the wind speeds increase with height above the surface), a survival configuration can be adopted. During extreme wind events, the frame of beams can be positioned horizontally ( $\alpha = 0$  deg), thus reducing the wind loads and positively impacting the structural performance [39,40].

### 2.2.2. Bifacial panels

Another strategy to maximize electricity generation is mounting bifacial panels rather than monofacial ones. These PV panels have a marginally lower cost and can absorb the surface-reflected irradiance, thus resulting in a higher energy yield to a reduced cost. Stein et al. [41] reported bifacial gains close to 30% for a ground-mounted dual-axis tracker. As for FPV systems, Tina et al. [30] reported bifacial gains of up to 13.5% for panels with a fixed tilt angle. However, these results should be considered with caution, as the benefits from bifacial panels in FPV systems are still unclear and may be limited by a lower reflectance of water surfaces with respect to land surfaces [42].

On most surfaces, light is reflected in a diffuse manner, which is why the irradiance resulting from surface reflection is referred to as diffuse irradiance. It is a function of the beam normal irradiance and sun zenith angle, sky diffuse irradiance, and surface reflectance – i.e., albedo, which depends on the properties of the surface. There are abundant studies with a focus on the surface land albedo, while an accurate determination of the ocean surface albedo is still a matter of research. In the absence of measured data of reflected radiation from water, a default albedo value of 0.2 is commonly assumed in the modelling of FPV systems [43]. However, recent research has suggested that using a default albedo value of 0.2 in the modelling of the reflected radiation of FPV systems tend to overestimate the total insolation [44]. According to climate observations and models, realistic values of the ocean mean surface albedo would be between 0.075 and 0.09 [45], ranging from 0.04 to 0.15 depending on the surface roughness (due to wind and waves) and on the solar incidence angle [42].

Not only the albedo, but the mounting conditions have a direct influence on the bifacial gains. For GPV systems, it is well-known that increasing the elevation of the installation reduces self-shading, which optimizes the performance of bifacial solar panels [46]. A similar benefit has also been reported for FPV systems [30]. In addition, the bifacial gains can be boosted by minimizing the obstructions to light reaching the panels from the back side [41]. HelioSea maximizes bifacial gains by elevating the PV panels to a significant height above the sea-surface. On these grounds, the beam frame layout should be optimized to avoid shadows casting on the rear (Fig. 5). In addition, the wave- and wind-induced translations of each unit in a solar farm demands large separations between units in the arrangement, which may be beneficial in terms of bifacial gains.

### 2.2.3. Cooling effects

A limitation of PV plants is their reduced efficiency during the hot season due to the thermal drift effect. Apart from the incident solar radiation itself, the cell operating temperature is determined by several environmental factors that affect the radiative and convective heat transfer. These are mainly the air temperature, the wind and, in case of FPV systems, the water temperature. Of course, this heat exchange is also influenced by the material properties of the panels and the mounting structure.

The water-cooling effect is commonly claimed a major advantage of FPV over ground-mounted PV systems and especially when the PV panels are mounted directly on a floating membrane, which allows thermal contact between panel and water [47]. However, while some authors have reported a water-cooling gain between 5 and 15% (e.g., [48]), others have reduced this value below 5% (e.g., [5,49]). It has also been suggested that the observed lower operating temperature for some FPV systems compared to GPV systems is predominantly due to local climate differences, since large water bodies provide lower ambient air temperatures and higher wind speeds than many land locations [49].

Given that the air-cooling effect intensifies as the wind speed increases, a greater impact is expected in oceanic environments compared to onshore areas. In addition, the wind speed increases with height because of the wind shear. By elevating solar panels above the water surface, HelioSea can benefit further from the air-cooling effect and reduce the operating cell temperature. This cooling gain can boost the efficiency as well as improve the long-term durability of solar panels [50].

### 2.3. Manufacturing, installation, and operation

One advantage of HelioSea is that it employs well-established elements and materials with standardized manufacturing techniques, thereby eliminating the need for any novel requirements or development in this regard. The concept is designed so that a single design can be used for locations with a wide range of climatic conditions. The latter does not apply to the mooring system, which must be adjusted based on the specific water depth of the installation site. This adaptability and standardization enable industrialization and the repetitive manufacturing of components to minimize the overall fabrication cost.

HelioSea is intended to resist multifaceted degradation mechanisms, including erosion, abrasion, UV-induced deterioration, extreme temperature fluctuations, elevated humidity, and, most importantly, salt-water corrosion. During fabrication, a meticulous surface preparation followed by a dual-layer protective system, involving hot-dip galvanization and an appropriate coating, must be applied to each steel member.

The TLP and the top-of-pole mount can be fabricated separately and joined at dockside before being taken offshore. Unlike offshore wind turbines, which require fabrication in port facilities due to the unaffordability of transporting their large components over land, the reduced dimensions and the rigid design of the system enable land transport from workshops outside of port facilities with lower rental costs, resulting in potential cost savings for manufacturing.

Once at port, HelioSea units are transported to the project site for installation. Conventionally, ballast water is used to increase the overall weight of TLPs, facilitating towing and anchoring operations. Prior to anchoring, the tendons are securely fastened to a foundation on a prepared seabed. Subsequently, de-ballasting is carried out to establish the necessary net buoyancy and tension in the tethers. This conventional installation process might present challenges due to the inherent free-floating instability associated with TLPs [22]. The reduced dimensions of HelioSea allow for consideration of shipping on a small-sized barge instead of towing. Alternatively, this technology can leverage procedures proposed for other TLPs (e.g., [51]). Regardless, conventional resources including small tugboats, cranes, and/or barges are required for commissioning, potentially resulting in significant cost efficiencies and simplification of marine operations.

### 3. Motion and structural analysis

This section presents an initial proof-of-concept that aims to assess the stability and structural behaviour of HelioSea under wave and wind action. Several load scenarios were defined, and a response analysis was conducted to structurally verify the main elements of the substructure. The rigid-body motions and the force system on the structure were solved in the time domain. Ansys Aqwa was used for this dynamic response analysis. This code has been widely applied in the field of marine renewable energy (e.g. to model wave energy converters [52]) and has already been applied to model other types of FPV structures [53]. The results of the response analysis were the inputs of the subsequent structural assessment of the substructure. The structural assessment of the superstructure lacks research interest since it has already been developed and applied in onshore solar trackers.

### 3.1. Testing design and conditions

The TLP allows multiple configurations and, therefore, an initial reference design had to be defined for testing. Tubular steel members were considered for the pontoons (rectangular cross section) and the mast (circular cross section), and steel wire ropes (6 × 36WS-IWRC made of AISI 316 steel [54]) were selected for the tethers. More detailed specifications for each component are included in Table 2. Although steel was considered for this analysis, future development may explore other materials such as fibre-reinforced polymers. Regarding the superstructure, it was modelled using a mass point and aerodynamic coefficients (defined in subsequent subsection). The structure has a total mass of 37.3 t, a draft of 11.5 m and a displacement of 74.5 m<sup>3</sup>.

HelioSea was analysed under operational and survival conditions representative of generic locations with a moderate climate (Table 3). A fixed orientation to the south of the vertical tracker ( $\beta = 0$  deg) and a constant water depth of  $d = 35$  m were assumed in both scenarios. Steady wind and regular waves were defined in terms of wind speed ( $U$ ), wave height ( $H$ ) and wave period ( $T$ ). In both operational and survival conditions, the wind direction ( $\theta$ ) was aligned to the wave direction ( $\delta$ ) to the north, opposing the vertical tracker. The latter was applied to maximize pitch motions, as they have the greatest impact on the electricity generation (as mentioned in Section 2.1.2). For operational conditions, the inclination of the horizontal tracker was set to  $\alpha = 40$  deg., while for survival conditions, the inclination was set to  $\alpha = 0$  deg.

### 3.2. Numerical method

The dynamics of the floating structure that make up the FPV system can be described with the following motion equation:

$$\mathbf{M}\ddot{\mathbf{x}} = \mathbf{f}_h + \mathbf{f}_M + \mathbf{f}_w + \mathbf{f}_m \quad (1)$$

with  $\mathbf{M}$ , the mass matrix of the structure;  $\mathbf{x}$ , the instantaneous position of the structure and  $\ddot{\mathbf{x}}$  its second time derivative (acceleration); and the following time-dependant forces on the structure:

- $\mathbf{f}_h(t)$ , the hydrostatic and restoring forces obtained as the balance between the gravitational forces  $\mathbf{f}_g(t)$  and the buoyant forces, for the instantaneous wet surface  $S(t)$ :

$$\mathbf{f}_h(t) = \mathbf{f}_g(t) + \rho g \int_{S(t)} p_s(t) \mathbf{n} dS \quad (2)$$

where  $p_s$  is the instantaneous static pressure.

- $\mathbf{f}_M(t)$ , the wave forces on the submerged elements. Regular wave conditions were simulated assuming the 2nd order Stokes wave

**Table 2**

Specifications of the main structural components: the mast, the pontoons and the tethers [54].

Component	Property [units]	Value
Mast	Length [m]	16.5
	Cross-section diameter [mm]	2000
	Thickness [mm]	20
	Material	Structural steel
	Yield strength [MPa]	275
Pontoons	Length [m]	6.0
	Section dimension [mm]	1000 × 1600
	Thickness [mm]	10
	Material	Structural steel
	Yield strength [MPa]	275
Tethers	Length [m]	23.5
	Nominal diameter [mm]	32
	Material	Stainless steel
	Linear density [kg/m]	4.2
	Stiffness [N/mm]	4800
	Breaking load [kN]	715

**Table 3**  
Definition of the test cases considered.

Parameter	Operational conditions	Survival conditions
Wind speed, $U$ [m/s]	5	30
Wind direction, $\theta$ [deg]	180	180
Wave height, $H$ [m]	1	4
Wave period, $T$ [s]	7	14
Wave direction, $\delta$ [deg]	180	180
Water depth, $d$ [m]	35	35
Vertical tracker, $\beta$ [deg]	0	0
Horizontal tracker, $\alpha$ [deg]	40	0

theory and both the substructure (mast and pontoons) and the tethers were considered slender and therefore non-diffracting (Fig. 6). On these grounds, the wave forces on the structure can be obtained by integrating the fluid forces on the cross section of each element by applying the Morison equation along with the extended Wheeler stretching method [55]. For a given cross section, the Morison equation reads

$$dF_M = \frac{1}{2} \rho \phi_D C_D |u_f - u_s| (u_f - u_s) + \rho \phi_A C_m \dot{u}_f - \rho \phi_A (C_m - 1) \dot{u}_s \quad (3)$$

with  $\rho$ , the water density;  $\phi_D$ , the characteristic drag diameter;  $C_D$ , the drag coefficient;  $u_f$ , the transverse directional fluid particle velocity;  $u_s$ , the transverse directional structure velocity;  $\phi_A$ , the element's cross-sectional area; and  $C_m$ , the inertia coefficient. Values of  $C_D = 0.75$  and  $C_m = 2$  were assumed in this work.

- $f_w(t)$ , the static wind forces on the superstructure, was estimated through the following formula [56]

$$f_w = \frac{1}{2} \rho U^2 S_{ref} C_f \quad (4)$$

where  $\rho$  is the air density,  $C_f$  is the overall force coefficient, and  $S_{ref}$  is the reference surface. The values of  $C_f$  varies with wind direction ( $\theta$ ) as well as with the inclination of the horizontal tracker ( $\alpha$ ). The values applied are summarized in Table 4.

- $f_m(t)$ , the forces in the mooring lines or tethers, modelled as linear cables through their stiffness, initial unstretched length (Table 2) and their corresponding attachment points: at the seabed and at the endpoints of each pontoon.

A time step of 0.01 s and a duration of 500 s were considered for the simulations. Once the all the forces were obtained for an instant of the time domain analysis, the dynamic problem was solved through Eq. (1). This is performed in Ansys Aqwa through a 2-stage predictor-corrector algorithm. In the first stage the forces on the structure are calculated as a function of time, position, and velocity. The position and velocity of the floating body for the next time step is then predicted in accordance with those forces. In the second stage, forces are obtained again as a function of the new values of position and velocity, which are corrected through Taylor's theorem. The structure adopts its new position, and the algorithm starts over.

**Table 4**  
Overall force coefficients for the superstructure [56].

Horizontal tracker, $\alpha$ [deg]	Wind direction, $\theta$ [deg]	Overall force coefficient, $C_f$
0	180	-0.5
40	180	-2.2

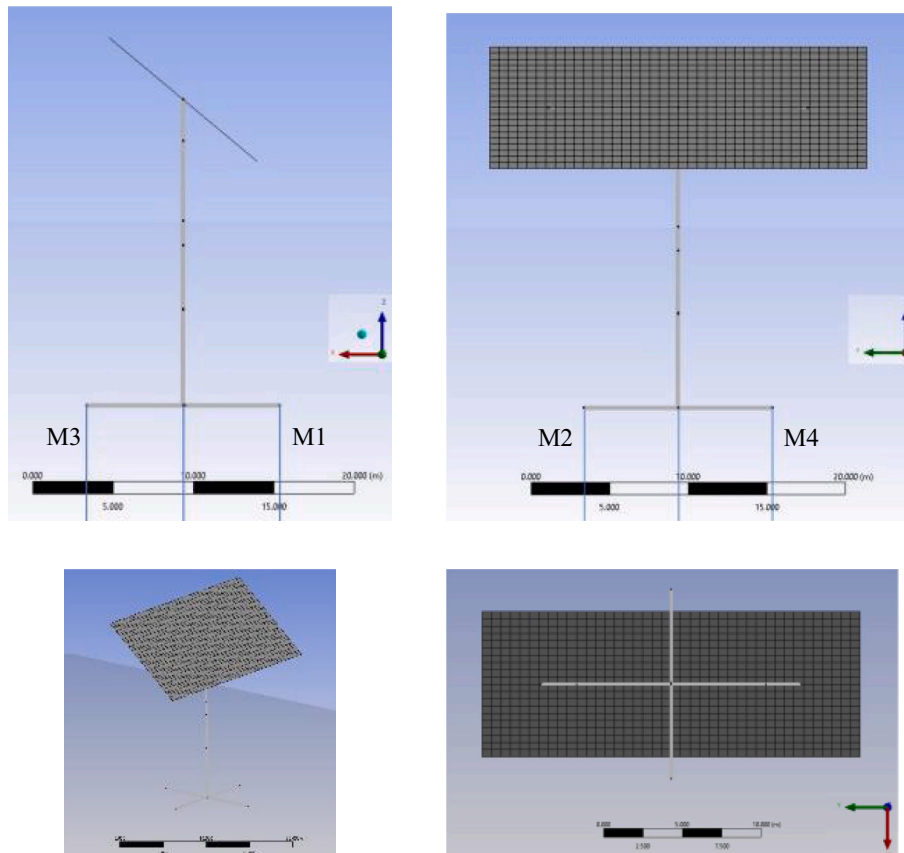


**Fig. 6.** Various perspectives of the model implemented in Ansys Aqwa numerical model.

### 3.3. Response analysis

Upon completion of the time domain analysis in Ansys Aqwa, results were retrieved in the form of time series of rigid body motions and structural forces. The motions in the 6 Degrees of Freedom (DoF) are shown in Fig. 7 for operational conditions. Negligible translational motions were obtained for sway and heave, as it could be expected for wind and wave directions in the x direction. The same applies for the rotational motions of roll and yaw. As for surge and pitch, the structure gets stabilized to a new equilibrium position within the first 100 s and, afterwards, it starts a harmonic oscillation with amplitudes of about 0.5 m and 0.1 deg., respectively. Excessive pitch motions may change the azimuth angle of the solar tracker and result in energy losses. Considering the low motions reached for operational conditions, significant misalignment of the solar PV panels is unlikely. It should be noticed that, for other wind and wave directions, the pitch values are expected to be even smaller. This result confirms HelioSea's capability to provide a stable platform for the installation of the PV panels and avoid losses associated to wave passing.

Fig. 8 shows the motions registered for survival conditions. Despite the increased motions in all DoF, sway, heave, roll, and yaw remain insignificant. Concerning surge and pitch, the structure oscillates around the new equilibrium position with amplitude of nearly 5 m and 0.6 deg., respectively. Note that, in contrast to rotations, the translations of the device have no impact on the performance of the solar panels. Furthermore, the analysis of losses caused by movements during survival conditions is of reduced relevance, given their infrequent occurrence. Nonetheless, it is worth noting the low value of pitch obtained even for survival conditions corresponding to a wave height of  $H = 5$  m and a wind speed of  $U = 30$  m/s.

The motions of the structure obtained for survival conditions can be considered to define a preliminary offshore solar farm layout. Assuming a maximum horizontal translation of 5 m for the device and taking into account that the horizontal projection of the proposed device spans 13.4 m, an estimate of the radius of the anchor swinging circle (depicted in Fig. 4) yields 18.4 m. Accordingly, an offshore solar farm with a hexagonal arrangement (a packing density of about 0.91) and 75-kW rated power units would present a capacity density – the ratio of the farm's rated capacity to its total area – of 64 MW/km<sup>2</sup>.

### 3.4. Structural assessment

Once obtained the characteristic loads from the time domain analysis, a global structural analysis was performed through classic beam theory and considering the characteristic resistance of the main components. The effects of shear deformations and rotatory inertia were ignored, and beam deflections were assumed sufficiently small. This approach was applied to the discretization of the Morison elements shown in Fig. 6. Normal stress, resulting from combining flexural and

axial stresses, along the main structural components was analysed. Shear and torsion presented negligible values and were omitted from the figure for the sake of simplicity. Bearing in mind the low TRL of HelioSea, no standards were considered for the structural assessment.

The critical section of the pontoons, concerning maximum normal stress was identified at the joint that connects the front pontoon (i.e., the pontoon moored to M3 in Fig. 6) with the mast. Accordingly, the critical section along the length of the mast corresponds to its base. Time series of the maximum normal stress in the critical sections of each element are presented in Fig. 9 for operational and survival conditions. It is important to note that, at different time steps, the maximum stress may correspond to various points along the height of a cross-section.

As expected, the normal stress levels increase substantially from operational to survival conditions. The upwind pontoon experiences stress levels reaching 70 MPa, while the mast's maximum stress level barely surpasses 25 MPa. The upwind pontoon experiences higher stress than the mast because of its lower inertia and cross-sectional area (according to the specifications provided in Table 2) and not because it is subjected to higher load levels.

Fig. 10 shows the time series of mooring forces for operational and survival conditions. Due to the symmetry of the structure in the direction of wind and waves, the results are identical for moorings M2 and M4. Consistent with the previous findings, the tether experiencing higher forces is M3, the one attached to the front of the structure (upwind). The maximum force in this line doubles from operational to survival conditions, increasing from about 145 kN to 300 kN. The forces on the other lines remain below 180 kN for both cases, being the line M1 (downwind) the one that experiences lower force levels. To this regard, one of the design conditions of the tethers is to prevent abrupt snapping, thereby safeguarding their structural integrity and averting sudden failures that could jeopardize the safety and stability of the entire system. As observed, even under survival conditions and considering the line M1, there is a consistent minimum load of 25 kN, which serves to keep the mooring lines from becoming slack and subsequently avoiding any subsequent snapping.

In general, all the structural components withstood the survival conditions with a sufficient safety margin, as indicated by the global safety factors displayed in Table 5. This result suggests that there is room for an optimization of the cross sections of the main structural elements of the substructure, which would result in a lower manufacturing cost (a first estimation is included in subsequent section). A strict safety factor of 2 was found for the mooring lines, which would require a larger cross section. In any case, further structural assessment is required, and engineering codes and standards should be applied.

## 4. Levelized cost of energy

A first approximation to the levelized cost of energy (LCOE) of a 75-kW rated power device is presented in this section. The environmental

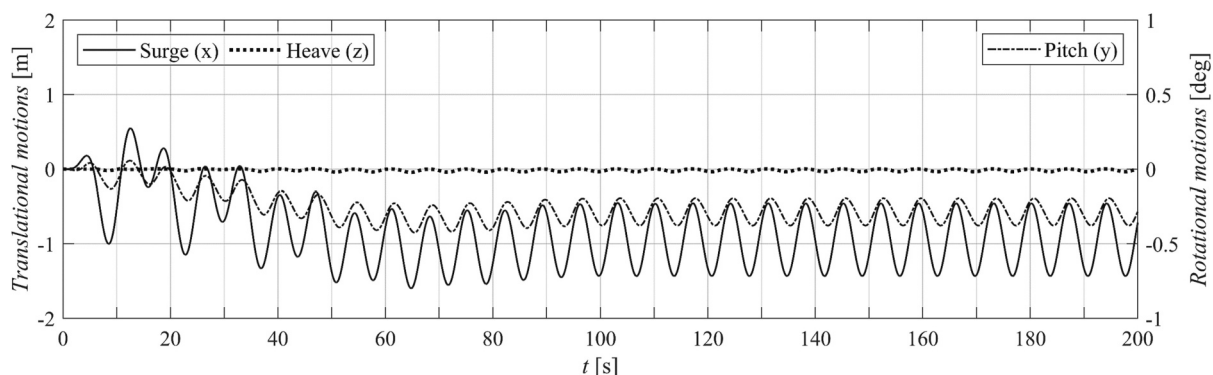


Fig. 7. Motions in the 6 Degrees of Freedom (DoF) for operational conditions.

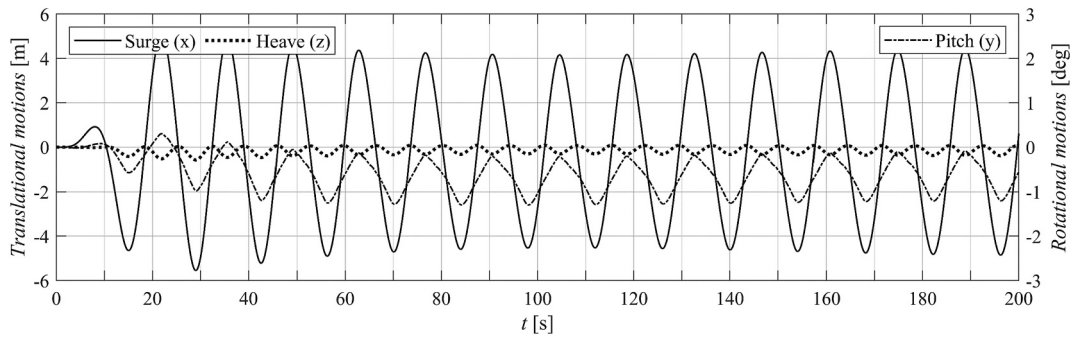


Fig. 8. Motions in the 6 Degrees of Freedom (DoF) for survival conditions.

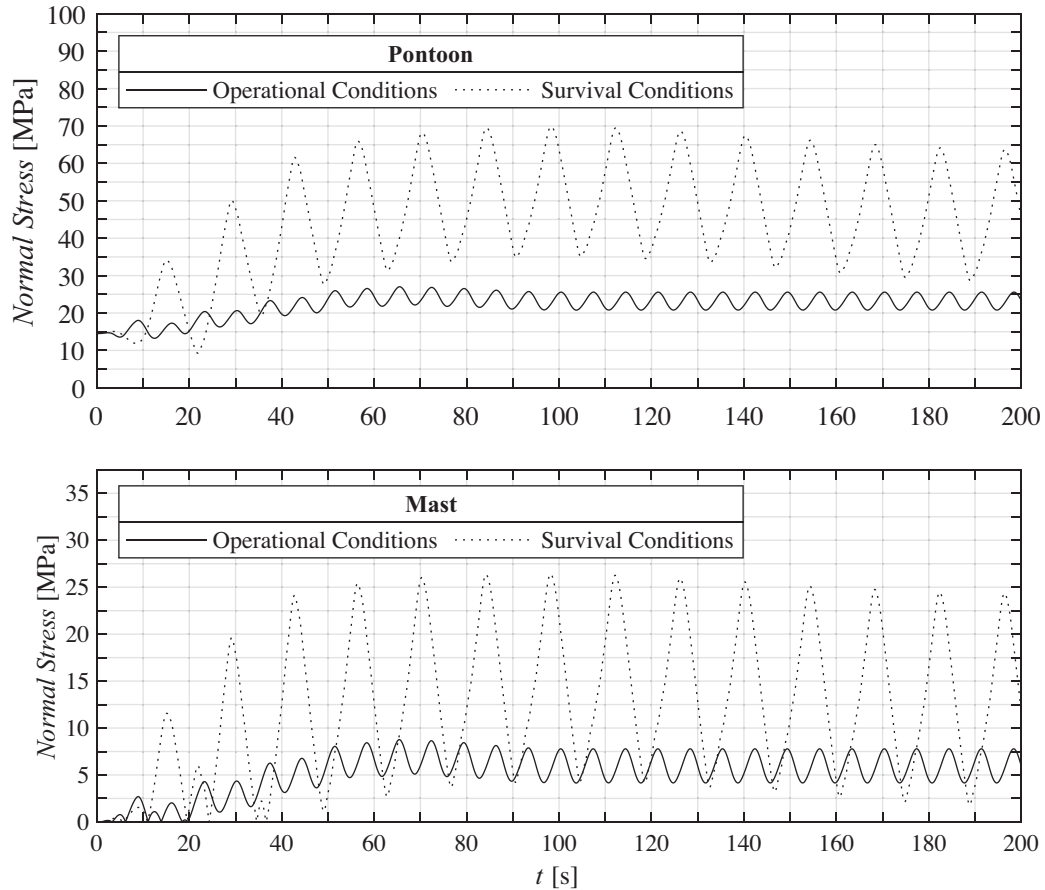


Fig. 9. Maximum normal stress at the critical sections of the pontoons and the mast (absolute values).

conditions of the Port of Vigo (Fig. 11) were considered for the assessment of the electricity generation. This selection was made based on its favourable environmental conditions for the future demonstration of the device. Its latitude ensures high irradiance levels throughout the year and its 14,000 ha of calm waters permit the deployment of an offshore solar farm in a moderate wave climate [57].

#### 4.1. Production assessment

For the estimation of the electricity production, PVGIS was used [58]. This tool is provided online by the European Joint Research Centre and delivers information about solar radiation and offers several key features for accurate PV system performance predictions [59].

The efficiency of photovoltaic modules depends on the module temperature ( $T$ ) and the solar irradiance ( $G$ ). Generally, efficiency decreases with increasing air temperature ( $T_a$ ), and the irradiance. In this

approach, the wind cooling effect is also considered. PVGIS uses a model proposed by Faiman [60] to calculate the module temperature:

$$T = T_a + \frac{G}{U_0 + U_1 \cdot W} \quad (5)$$

where  $W$  is the wind speed and  $U_0$  and  $U_1$  are empirical coefficients [61].

The rated power of solar modules is commonly defined under standardized conditions known as Standard Test Conditions (STC), established by the IEC-60904-1 standard. These conditions correspond to an irradiance of  $G_{STC} = 1000 \text{ W/m}^2$ , a module temperature of  $T_{STC} = 25 \text{ }^\circ\text{C}$ , and a light spectrum similar to that of a sunny day with the sun at about  $40^\circ$  above the horizon and the module tilted about  $40^\circ$  towards the sun [62].

PVGIS computes the power output of the PV modules using the model proposed by Huld et al. [63]:

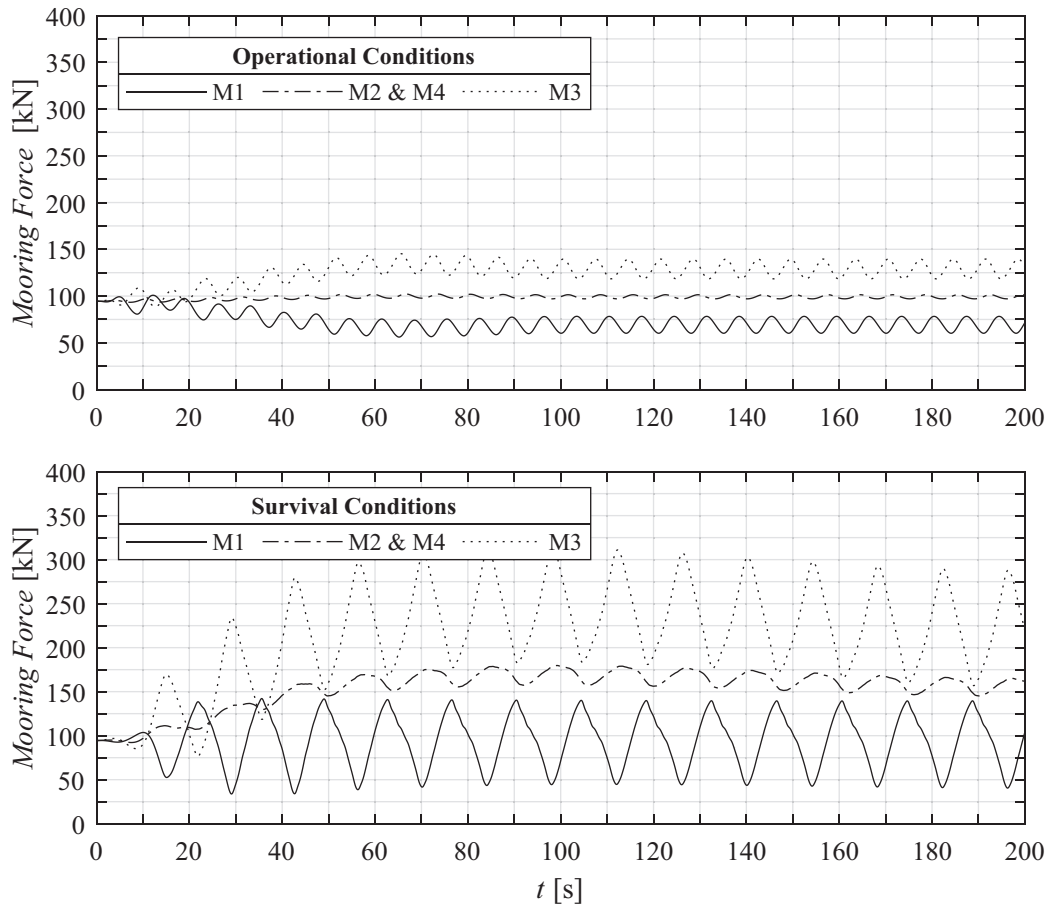


Fig. 10. Mooring forces for operational and survival conditions.

Table 5  
Global safety factors of the main components for survival conditions.

Element	Verification [units]	Maximum value	Safety factor
Mast	Bending - axial [MPa]	26.4	10
Mast	Shear - torsion [kN]	95.0	133
Pontoon	Bending - axial [MPa]	69.9	4
Pontoon	Shear - torsion [kN]	242.7	20
Tether	Maximum load [kN]	312.0	2.3

$$P = GAeff_{nom}eff_{rel}(G, T^i) \tag{6}$$

with  $G^* = G/G_{STC}$ ;  $A$ , the surface of the PV panels;  $T = T - T_{STC}$ ;  $eff_{nom} = 0.85$ , the module nominal efficiency; and  $eff_{rel}$  the relative efficiency compared to STC conditions given by:

$$eff_{rel}(G, T) = 1 + k_1 \ln(G) + 2k_2 \ln(G) + k_3 T + k_4 T \ln(G) + 2k_5 T \ln(G) + 2k_6 T^i \tag{7}$$

where  $k_i$ , for  $i = \{1, 2, \dots, 6\}$ , correspond to empirical coefficients

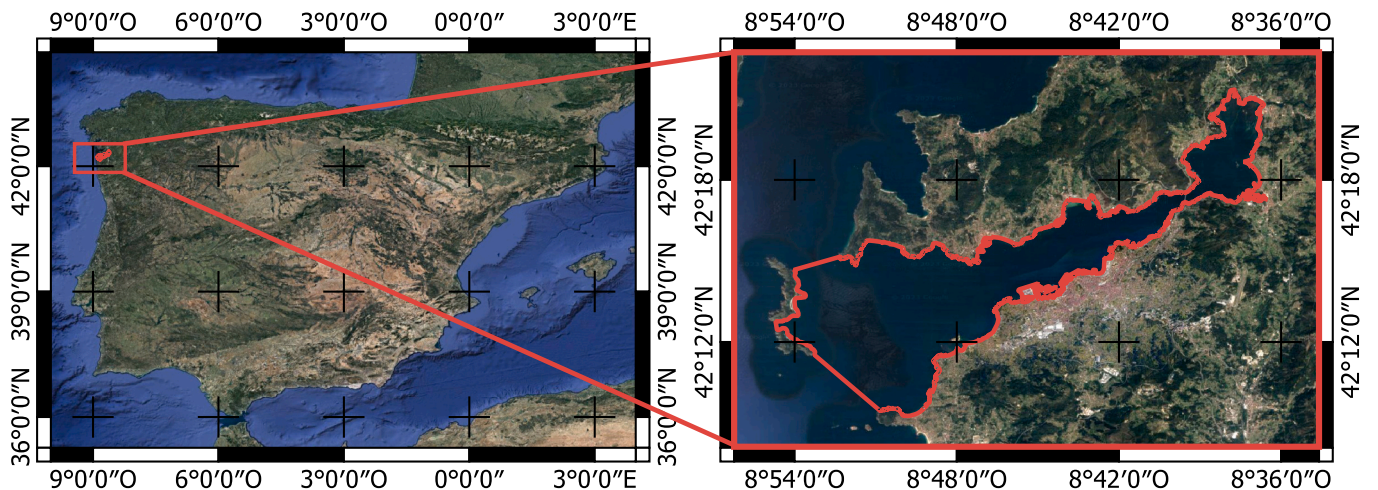


Fig. 11. Location of the Port of Vigo.

depending on the PV technology.

The value of  $P$  obtained with Eq. (6) corresponds to the power delivered by the module or array in the form of direct current (DC) and it should be converted into alternating current (AC) using an inverter. To account for the power losses in this conversion as well as in the cables, a 14% reduction in the power output was considered. Furthermore, the power output of PV modules tends to decrease over its lifespan, thus a loss of 0.5% of rated power per year of operation is typically considered [64].

Assuming a lifetime of  $n = 20$  years, an average annual electric energy generation of 154.62 MWh was achieved. It is important to highlight that this value may be conservative since bifacial gains were excluded in the analysis. Moreover, the cooling effects estimated by PVGIS are derived from onshore locations and may underestimate the benefits of offshore sites, where the presence of water and stronger winds is expected to amplify this effect.

#### 4.2. Levelized cost of energy (LCOE)

The Levelized Cost of Electricity (LCOE) was calculated by dividing the entire lifecycle cost by the cumulative electricity generation using the formula [65]:

$$LCOE = \frac{CAPEX + \sum_{t=1}^n \frac{OPEX}{(1+r)^t}}{\sum_{t=1}^n \frac{E}{(1+r)^t}} \quad (8)$$

where:

- CAPEX represents the capital expenditure, accounting for the investment in construction and commissioning.
- OPEX stands for the operation and maintenance expenditure, covering the total annual operating cost per year  $t$  over the FPV lifetime.
- $r$  denotes the discount rate.
- $E$  is the electric energy yield obtained by applying Eq. (6) for year  $t$ .

Factors such as residual value, decommissioning costs, taxes, subsidies/incentives, and interest during construction were neglected. A value of  $r = 7.5\%$  was considered, taking into account the weighted

average cost of capital (WACC) for countries like Spain within the Organisation for Economic Co-operation and Development (OECD) [66].

The offshore FPV sector is still in its early stages of development and its costs are not well-established, in contrast to the more mature GPV sector and, to a lesser extent, offshore wind energy technologies. To address this uncertainty, reference minimum and maximum costs were established to define optimistic and conservative values for the LCOE. Some material cost estimates considered industry experience and prevailing market prices, while in some cases, data from previous studies were assumed.

CAPEX was divided into substructure, superstructure, and commissioning expenses as shown in Table 6. In the substructure, the costs per unit of the mast and the pontoons were estimated by considering current market prices and including the structural steel, the required protective system (detailed in Section 2.3), the labour hours, welding, and bending. A higher cost for the mast was anticipated based on experience.

For the mooring system, the cost of the wire ropes in the tethers was assumed in the range between 0.02 and 0.09 € per meter of length and kilonewton of minimum breaking load [67]. With a breaking load of 715 kN (Table 2), this results in a cost range between 14.30 and 64.35 €/m. Four gravity base anchors of concrete, each weighing about 23 t, were considered along with a market cost for concrete ranging between 36 and 52 €/t.

A unique value for the cost of the tracking mechanism was considered based on the previous study of Bahrami et al. on this topic [68]. The cost of the electrical components and commissioning were obtained from already existing GPV tracking systems, taking as a reference the minimum and maximum costs from references [69,70], respectively.

OPEX was obtained as the sum of the operation & maintenance (O&M) costs, the insurance costs (IC) and the inverter warranty extensions (IEI). The minimum O&M cost was obtained by applying a fixed rate of  $10.34 \cdot 10^{-3}$  € per Watt of rated power [66], and the maximum was obtained as 11% of the electricity generation [71]. In addition, a 2% annual increase rate in O&M costs was applied to account for material aging, based on previous experience with GPV [66]. The minimum for the sum of IC and IEI was defined by applying  $1.4 \cdot 10^{-3}$  € per Watt of rated power [66], and its maximum as the 1.42% of CAPEX [72].

Once applied all the abovementioned values, it results a LCOE in the

**Table 6**  
Maximum and minimum reference costs used in CAPEX estimates.

	Component	[units]	Measurement	Per-unit [€]		Total [€]	
				min.	max.	min.	max.
Substructure	Mast	[kg]	16,000.00	3.50	5.00	56,000.00	80,000.00
	Pontoons	[kg]	9700.00	3.00	4.00	29,100.00	38,800.00
	Tethers	[m]	94.00	14.30	64.35	1344.20	6048.90
	Gravity base anchors	[t]	91.74	36.00	52.00	3302.75	4770.64
					Subtotal	89,746.95	129,619.54
Superstructure	Frame	[kg]	7611.80	7.00	10.00	53,282.60	76,118.00
	Tracking mechanism	-	1.00	4500.00	4500.00	4500.00	4500.00
	Solar panels	units	138.00	217.39	260.87	30,000.00	36,000.00
	Electrical components	-	1.00	4512.60	12,785.70	4512.60	12,785.70
				Subtotal	92,295.20	129,403.70	
Commissioning		-	1.00	10,529.40	15,042.00	10,529.40	15,042.00
					CAPEX	192,571.55	274,065.24

**Table 7**  
Levelized cost of energy (LCOE) range for different renewable energy sources.

Renewable energy	Lower LCOE [€/MWh]	Ref.	Upper LCOE [€/MWh]	Ref.
Ground-mounted photovoltaic (GPV)	35	[5]	40	[5]
Onshore floating photovoltaic (FPV)	50	[5]	96	[5]
Floating offshore wind	95	[13]	160	[13]
Wave	225	[16]	1750	[16]
Tidal	255	[16]	910	[16]
HelioSea	160	-	270	-

range between 160 and 270 €/MWh. Table 7 compares these estimates with those for other renewable systems. The cost of energy for HelioSea would be four to six times that of GPV and two to three times that of onshore FPV, both mature technologies. Nonetheless, the proposed offshore FPV system becomes highly competitive when compared to other marine renewable resources. Its LCOE would be less than twice the corresponding for floating offshore wind, a technology with a higher TRL than the proposed concept. Moreover, if compared to wave and tidal, HelioSea presents a much lower cost of energy.

These results demand careful consideration due to the large uncertainties and the assumptions made during the LCOE analysis. The characteristics of the installation site may significantly influence the estimates. On another note, there is substantial room for optimizing HelioSea, currently at its proof-of-concept stage, which could potentially lead to a reduction in CAPEX. Furthermore, the advantages of this device in terms of commissioning have not been thoroughly addressed yet. In summary, while the results offer optimism and serve as a reference basis for future developments, it is essential to approach them with caution.

## 5. Conclusions

HelioSea, a novel floating concept for harnessing solar energy offshore, combines two key features: a dual-axis tracking system and a TLP. Although the former is a technology that has been commonly applied in GPV installations, the TLP has never been proposed before in the design of FPV systems. This design seeks a dual objective: maximizing the electricity generation and providing a reliable structure to survive the challenging marine environment. A comprehensive analysis of the advantages and disadvantages of this system was presented for the first time. A motion and structural analysis was performed through hydrodynamic numerical modelling, followed by an economic evaluation in terms of the LCOE.

The dual-axis tracker maximizes the amount of direct normal irradiance striking the front of the array throughout the year. This special design also allows increasing the height of the solar modules above the water surface to avoid wave slamming and splashing. In terms of production, this feature may not only result in an increase of the cooling effect, but also in the levels of reflected irradiance that reach the bifacial solar modules. On the contrary, the higher wind exposure may compromise the superstructure, which is why HelioSea incorporates a survival configuration wherein the panels are positioned horizontally to minimize wind loading.

The TLP provides stability to the whole structure and, in conjunction with the slender design of the mast, minimizes wave loading. The mooring system ensures minimal variations in the azimuth and tilt angles of the PV panels, critical for efficient solar energy conversion. Under operational conditions (wave height,  $H = 1$  m, and wind speed,  $U = 5$  m/s), pitch motion was negligible in terms of generation, with amplitudes of 0.1 deg. Even under survival conditions ( $H = 5$  m and  $U = 30$  m/s), pitch motion remained minimal, with amplitudes of 0.6 deg. Although rotations were controlled, a large surge amplitude of 5 m was observed under survival conditions. While translations do not affect the efficiency of solar energy conversion, they do impact the required safety distance between units. An offshore solar plant with 75-kW rated power HelioSea units, and a hexagonal packing arrangement would present a capacity density of 64 MW/km<sup>2</sup>.

The structural assessment revealed robust safety factors for the majority of elements in the substructure. Nonetheless, the tethers and the pontoons demonstrated lower safety factors of 2.3 and 4, respectively. These outcomes, derived from an initial design that lacks optimization, confirm the overall order of magnitude of the substructure dimensions. Furthermore, it is anticipated that some structural elements may undergo section reduction in future development.

The LCOE assessment, considering uncertainties and assuming reference costs from various technologies, places HelioSea in the range of 160 to 270 €/MWh. While these values diverge significantly from

those of ground-mounted solar systems, they align with a comparable order of magnitude to offshore floating wind systems and are notably lower than other marine renewable energies, such as wave and tidal energy.

In summary, HelioSea introduces distinctive features, facilitating the transition of FPV technology to offshore environments. While recognizing areas for improvement, the promising results justify additional exploration through numerical and experimental techniques. Subsequent efforts should focus on optimizing geometry, materials, and energy costs, encompassing a broader range of environmental conditions, utilizing advanced numerical tools, and adhering to standardized structural assessments.

## CRediT authorship contribution statement

**Mario López:** Writing – review & editing, Writing – original draft, Supervision, Project administration, Methodology, Investigation, Funding acquisition, Formal analysis, Conceptualization. **Rubén Claus:** Writing – review & editing, Writing – original draft, Visualization, Software, Project administration, Methodology, Investigation, Formal analysis, Conceptualization. **Fernando Soto:** Writing – original draft, Visualization, Software, Methodology, Investigation, Conceptualization. **Zenaida A. Hernández-Garrastacho:** Writing – original draft, Methodology, Investigation, Formal analysis, Conceptualization. **Alejandro Cebada-Relea:** Visualization, Software, Formal analysis. **Orlando Simancas:** Supervision, Resources, Project administration, Investigation, Conceptualization.

## Declaration of competing interest

The authors declare that they have no known competing financial interests or personal relationships that could have appeared to influence the work reported in this paper.

## Data availability

Data will be made available on request.

## Acknowledgments

This work was supported by the PORTOS project co-financed by the Interreg Atlantic Area Programme through the European Regional Development Fund [grant number EAPA\_784/2018]. During this work, R. Claus was supported by the “Programa Severo Ochoa de Ayudas para la investigación y docencia”, a research fellowship programme financed by the Government of the Principality of Asturias (Spain) [grant number AYUD0029T01]; and A. Cebada was supported by the “Ayudas para realización de Tesis Doctorales. Modalidad A: Contratos de Investigación en régimen de concurrencia competitiva”, a research fellowship programme financed by the University of Oviedo (Spain) [grant number PAPI-21-PF-31].

## References

- [1] de Paulo AF, Porto GS. Evolution of collaborative networks of solar energy applied technologies. *J Clean Prod* 2018;204:310–20.
- [2] Kabir E, Kumar P, Kumar S, Adelodun AA, Kim K-H. Solar energy: potential and future prospects. *Renew Sustain Energy Rev* 2018;82:894–900.
- [3] Turney D, Fthenakis V. Environmental impacts from the installation and operation of large-scale solar power plants. *Renew Sustain Energy Rev* 2011;15(6):3261–70.
- [4] Rosa-Clot M, Tina GM. Current status of FPV and trends. In: *Floating PV plants*. Academic Press; 2020. p. 9–18.
- [5] Oliveira-Pinto S, Stokkermans J. Assessment of the potential of different floating solar technologies—Overview and analysis of different case studies. *Energy Convers Manage* 2020;211:112747.
- [6] Cazzaniga R, Cicu M, Rosa-Clot M, Rosa-Clot P, Tina GM, Ventura C. Floating photovoltaic plants: performance analysis and design solutions. *Renew Sustain Energy Rev* 2018;81:1730–41.

- [7] Liu H, Krishna V, Lun Leung J, Reindl T, Zhao L. Field experience and performance analysis of floating PV technologies in the tropics. *Prog Photovoltaics Res Appl* 2018;26(12):957–67.
- [8] Farrar LW, Bahaj ABS, James P, Anwar A, Amdar N. Floating solar PV to reduce water evaporation in water stressed regions and powering water pumping: case study Jordan. *Energy Convers Manage* 2022;260:115598.
- [9] Haas J, Khalighi J, de la Fuente A, Gerbersdorf SU, Nowak W, Chen PJ. Floating photovoltaic plants: ecological impacts versus hydropower operation flexibility. *Energy Convers Manage* 2020;206:112414.
- [10] López M, Soto F, Hernández ZA. Assessment of the potential of floating solar photovoltaic panels in bodies of water in mainland Spain. *J Clean Prod* 2022;340:130752.
- [11] Trapani K, Millar DL. Proposing offshore photovoltaic (PV) technology to the energy mix of the Maltese islands. *Energy Convers Manage* 2013;67:18–26.
- [12] Temiz M, Dincer I. Techno-economic analysis of green hydrogen ferries with a floating photovoltaic based marine fueling station. *Energy Convers Manage* 2021;247:114760.
- [13] Martínez A, Iglesias G. Mapping of the levelized cost of energy for floating offshore wind in the European Atlantic. *Renew Sustain Energy Rev* 2022;154:111889.
- [14] López M, Rodríguez N, Iglesias G. Combined floating offshore wind and solar PV. *J Mar Sci Eng* 2020;8(8).
- [15] Rosa-Santos P, Taveira-Pinto F, López M, Rodríguez CA. Hybrid Systems for Marine Energy Harvesting. *J Mar Sci Eng* 2022;10(5).
- [16] Taveira-Pinto F, Rosa-Santos P, Fazeres-Ferradaso T. Marine renewable energy. *Renew Energy* 2020;150:1160–4.
- [17] Grech M, Stagno LM, Aquilina M, Cadamuro M, Witzke U. Floating photovoltaic installations in Maltese sea waters. In: *Proceedings of the 32nd European Photovoltaic Solar Energy Conference and Exhibition, Munich, Germany*; 2016. p. 20–4.
- [18] Claus R, López M. Key issues in the design of floating photovoltaic structures for the marine environment. *Renew Sustain Energy Rev* 2022;164:112502.
- [19] SeaVolt. *Catching the new energy wave* [Online]. Available: <https://www.seavolt.be/>; 2023 [Accessed: 29-Apr-2023].
- [20] Uzunoglu E, Chen B, Soares CG. Stress distribution on the preliminary structural design of the CENTEC-TLP under still water and wave-induced loads. 2023.
- [21] Chandrasekaran S. *Dynamic analysis and design of offshore structures vol. 761*. Springer; 2015.
- [22] Jiang Z. Installation of offshore wind turbines: a technical review. *Renew Sustain Energy Rev* 2021;139:110576.
- [23] Kausche M, Adam F, Dahlhaus F, Großmann J. Floating offshore wind - economic and ecological challenges of a TLP solution. *Renew Energy* 2018;126:270–80.
- [24] Ma C, Liu Z. Water-surface photovoltaics: performance, utilization, and interactions with water eco-environment. *Renew Sustain Energy Rev* 2022;167(August 2020):112823.
- [25] Trapani K, Millar DL. The thin film flexible floating PV (TFP-PV) array: the concept and development of the prototype. *Renew Energy Nov*. 2014;71:43–50.
- [26] Jiang Z, et al. Design and model test of a soft-connected lattice-structured floating solar photovoltaic concept for harsh offshore conditions. *Mar Struct* 2023;90(July 2022).
- [27] Solar Duck. *Unique Solution Solar Duck* [Online]. Available: <https://solarduck.tech/unique-solution/> [Accessed: 01-Oct-2023].
- [28] Lee TD, Ebong AU. A review of thin film solar cell technologies and challenges. *Renew Sustain Energy Rev* 2017;70:1286–97.
- [29] Cebada-Relea AJ, López M, Aenlle M. Time-domain numerical modelling of the connector forces in a modular pontoon floating breakwater under regular and irregular oblique waves. *Ocean Eng* 2022;243:110263.
- [30] Tina GM, Bontempo Scavo F, Merlo L, Bizzarri F. Comparative analysis of monofacial and bifacial photovoltaic modules for floating power plants. *Appl Energy* 2021;281:116084.
- [31] Bugeja R, Stagno L Mule, Branche N. The effect of wave response motion on the insolation on offshore photovoltaic installations. *Sol Energy Adv* 2021;1:100008.
- [32] Lin Z, Liu X. Sustainable development of decommissioned FPSO as a floating solar plant—case study of the effects of tilt angle on energy efficiency. In: *Proceedings of the International Conference on Applied Energy, Västerås, Sweden*. 15; 2019.
- [33] Diendorfer C, Haider M, Lauermann M. Performance analysis of offshore solar power plants. *Energy Procedia* 2014;49:2462–71.
- [34] Eke R, Senturk A. Performance comparison of a double-axis sun tracking versus fixed PV system. *Sol Energy* 2012;86(9):2665–72.
- [35] Choi YK, Lee YG. A study on development of rotary structure for tracking-type floating photovoltaic system. *Int J Precis Eng Manuf* 2014;15(11):2453–60.
- [36] Campana PE, Wästhage L, Nookuea W, Tan Y, Yan J. Optimization and assessment of floating and floating-tracking PV systems integrated in on- and off-grid hybrid energy systems. *Sol Energy Jan*. 2019;177:782–95.
- [37] Nsengiyumva W, Chen SG, Hu L, Chen X. Recent advancements and challenges in solar tracking systems (STS): a review. *Renew Sustain Energy Rev* 2018;81:250–79.
- [38] Awasthi A, et al. Review on sun tracking technology in solar PV system. *Energy Rep* 2020;6:392–405.
- [39] Oliveira-Pinto S, Stokkermans J. Marine floating solar plants: an overview of potential, challenges and feasibility. *Proc Inst Civ Eng Marit Eng* 2020;173(4):120–35.
- [40] DNV AS. *DNV-RP-C205: Environmental conditions and environmental loads*. 2019.
- [41] Stein JS, Riley D, Lave M, Hansen C, Deline C, Toor F. Outdoor field performance from bifacial photovoltaic modules and systems. In 2017 IEEE 44th photovoltaic specialist conference (PVSC) (pp. 3184–3189). p. 3184–9.
- [42] Rosa-Clot M, Tina GM. *Submerged and floating photovoltaic systems: modelling, design and case studies*. Academic Press; 2017.
- [43] Patel SS, Rix AJ. Water surface Albedo modelling for floating Pv plants. In: *6th South. African Sol Energy Conf*, no. November 2019; 2019.
- [44] Patel SS, Rix AJ. The impact of water surface albedo on incident solar insolation of a collector surface. In: *2020 Int. SAUPEC/RobMech/PRASA Conf SAUPEC/RobMech/PRASA*; 2020.
- [45] Wild M, et al. The energy balance over land and oceans: an assessment based on direct observations and CMIP5 climate models. *Climate Dynam* 2015;44(11–12):3393–429.
- [46] Sun X, Khan MR, Deline C, Alam MA. Optimization and performance of bifacial solar modules: a global perspective. *Appl Energy* 2018;212:1601–10.
- [47] Kjeldstad T, Lindholm D, Marstein E, Selj J. Cooling of floating photovoltaics and the importance of water temperature. *Sol Energy* 2021;218:544–51.
- [48] Kamuyu WCL, Lim JR, Won CS, Ahn HK. Prediction model of photovoltaic module temperature for power performance of floating PVs. *Energies* 2018;11(2).
- [49] Kjeldstad T, et al. The performance and amphibious operation potential of a new floating photovoltaic technology. *Sol Energy* 2022;239:242–51.
- [50] Sun X, Silverman TJ, Zhou Z, Khan MR, Bermel P, Alam MA. Optics-based approach to thermal management of photovoltaics: selective-spectral and radiative cooling. *IEEE J Photovoltaics* 2017;7(2):566–74.
- [51] Myland T, Adam F, Dahlhaus F, Großmann J. Towing tests for the GICON®-TLP for offshore wind turbines. In: *Renew. Energies Offshore - 1st Int. Conf. Renew. Energies Offshore, RENEW 2014*; 2015. p. 705–8.
- [52] Giannini G, López M, Ramos V, Rodríguez C.A., Rosa-Santos P., Taveira-Pinto F. Geometry assessment of a sloped type wave energy converter. *Renew Energy*, 171: 672–686.
- [53] Claus R, López M. A methodology to assess the dynamic response and the structural performance of floating photovoltaic systems. *Sol Energy* 2023;262:111826.
- [54] Lankhorst. *Lankhorst Ropes* [Online]. Available, <https://www.lankhorstropes.com/>; 2023 [Accessed: 01-Oct-2023].
- [55] Wheeler JD. Method for calculating forces produced by irregular waves. *Proc Annu Offshore Technol Conf* 1969;1969-May(03):71–9.
- [56] Standard B. *Eurocode 1: Actions on structures*. 2010.
- [57] López M, Claus R, Soto F, Cebada A. Structural reliability of a novel offshore floating photovoltaic system to supply energy demands of ports. 2018.
- [58] Joint Research Centre - European Commission. *Photovoltaic Geographical Information System (PVGIS)* [Online]. Available, <http://re.jrc.ec.europa.eu/pvgis.html> [Accessed: 01-Oct-2023].
- [59] Huld T, Müller R, Gambardella A. A new solar radiation database for estimating PV performance in Europe and Africa. *Sol Energy* 2012;86(6):1803–15.
- [60] Faiman D. Assessing the outdoor operating temperature of photovoltaic modules. *Prog Photovoltaics Res Appl* 2008;16(4):307–15.
- [61] Koehl M, Heck M, Wiesmeier S, Wirth J. Modeling of the nominal operating cell temperature based on outdoor weathering. *Sol Energy Mater Sol Cells Jul*. 2011;95(7):1638–46.
- [62] Muneer Tariq. Solar radiation model for Europe. *Build Serv Eng Res Technol* 1987:153–63.
- [63] Huld T, et al. Solar energy materials & solar cells a power-rating model for crystalline silicon PV modules. *Sol Energy Mater Sol Cells* 2011;95(12):3359–69.
- [64] Jordan DC, Kurtz SR. Photovoltaic degradation rates—an analytical review. *Prog Photovoltaics Res Appl* 2013;21(1):12–29.
- [65] Kost C, et al. Levelized cost of electricity: PV and CPV in comparison to other technologies. *Fraunhofer Ise*; 2013.
- [66] IRENA. *Renewable generation costs in 2022*. 2022.
- [67] Umama EC, Tamunodukobipi DTI, Inegiyemiema M. Design of mooring system for a floating production storage and offloading (FPSO) terminal. *Glob J Eng Technol Adv* 2021;7(1):019–32.
- [68] Bahrami A, Okoye CO, Atikol U. Technical and economic assessment of fixed, single and dual-axis tracking PV panels in low latitude countries. *Renew Energy* 2017;113:563–79.
- [69] World Bank Group, ESMAP, and SERIS. *Where Sun Meets Water: Floating Solar Handbook for Practitioners*. 2019.
- [70] Stein JS, Farnung B. PV performance modeling methods and practices - results from the 4th PV performance modelling collaborative workshop. 2017.
- [71] Copernicus Climate Change Service. *Offshore wind farm operations and maintenance*. National Taiwan University of Science and Technology / Universitat Politècnica De Catalunya; 2022.
- [72] Shafiee M, Brennan F, Espinosa IA. A parametric whole life cost model for offshore wind farms. *Int J Life Cycle Assess* 2016;21(7):961–75.